doi:10.1246/cl.2011.1210
1210 Published on the web October 26, 2011

Highlight Review

Recent Progress in Chemical Characterization of Supported Gold Catalysts: CO Adsorption on Au/Ceria–Zirconia

Juan J. Delgado, José M. Cíes, Miguel López-Haro, Eloy del Río, José J. Calvino, and Serafín Bernal*

(Received July 15, 2011; CL-118011)

Abstract

An approach correlating quantitative CO adsorption data with the nanostructural properties of Au/CeO_2–ZrO_2 catalysts is discussed. It has been used to show that the CO adsorption occurs on Au sites with coordination number ≤ 7, that Au dispersion has a dramatic influence on the amount of CO strongly chemisorbed on the support, and that a fully reversible SMSI effect may be induced by successive mild reduction and reoxidation treatments.

1. Introduction

The discovery in 1987 by Haruta et al.[1] that gold highly dispersed on appropriate oxide supports shows much higher CO oxidation activity than the analogous systems constituted by noble metals of Groups 8–10 represents a major breakthrough point in the history of the catalysis by gold.[2] Following this, in principle, unexpected finding,[3] a dramatic increase in the number of published papers on gold catalysts has been observed.[4] Despite the big research effort devoted to this topic, many important questions about the ultimate origin of the exceptional behavior of gold remain open to discussion.[5]

The adsorption of the reactant molecules is acknowledged to be a key initial step of the heterogeneous catalytic processes. Accordingly, to gain detailed information about the surface chemistry of gold is certainly a relevant issue in order to arrive at a finer understanding of its catalytic behavior. As recently stressed,[2] until some 20 years ago, very little information was available on the chemisorptive properties of gold, the extreme nobility which was traditionally assumed to characterize this metal being invoked to justify this lack of studies. In the last two decades, however, the number of papers dealing with this topic has grown very rapidly,[2,6] a considerable amount of data being presently available. Though the adsorption of a relatively large number of molecules and atoms has been investigated,[6] CO is certainly one of the most commonly used probe molecules for gold surfaces.[2]

At present, the CO–Au interaction has been investigated on a variety of systems including massive single crystals,[6–12] small clusters or nanoparticles supported on both planar model,[13–24] and powdered oxides.[25–34] Studies on the CO interaction with gas-phase Au clusters have also been reported.[35–37] Depending on the specificities of the investigated systems, significantly different experimental conditions and techniques have been applied in the above-mentioned studies. Finally, CO adsorption on gold has also been investigated from a theoretical point of view.[14–16,38,39] From all these studies a number of relevant conclusions have already been obtained. Thus, with reference to the noble metals of Groups 8–10, gold interaction with CO is much weaker.[2,6] Consistently, it is generally acknowledged that the active sites for CO adsorption consist of defective, low-coordination, surface gold atoms.[2,6,22,40] This represents a first problem very much limiting the conventional use of CO as a tool for characterizing gold surfaces. In the case of supported gold catalysts, the simultaneous occurrence of CO adsorption on the support may constitute a second serious difficulty.[2] Therefore, in order to successfully use CO adsorption for characterizing supported gold catalysts, specific developments have to be made in order a) to make quantitative determination of the metal and support contributions to the total amount of adsorbed CO; b) to gain a deeper knowledge of the nanostructural characteristics of the surface gold atoms involved in the CO chemisorption process; c) to analyze the eventual role played by the dispersed metal phase in the CO adsorption on the support and, also very important in the case of catalysts including in their formulation reducible supports, d) to establish on a quantitative basis the influence of the redox state of the support on the adsorption capability of the Au nanoparticles.

In this work, an approach recently developed to overcome the problems mentioned above[41–43] is briefly reviewed. By combining in an appropriate manner experimental high-resolution transmission and high-angle annular dark field-scanning-transmission electron microscopy (HRTEM and HAADF-STEM), FTIR spectroscopy, and volumetric CO adsorption studies with nanostructural computer modeling techniques,[41] this approach has first been applied to a series of catalysts consisting of gold nanoparticles supported on ceria–zirconia (CZ) and closely related mixed oxides.[41–43] This is a relatively new family of materials which has received increasing attention because of its outstanding activity in a number of relevant catalytic reactions having in common the participation as reactant of the CO molecule.[44–51] Herein, special attention will be paid to the discussion of the chemical information that can be obtained from the correlation of the CO adsorption data with the nanostructural properties of the corresponding catalysts.

*Juan J. Delgado, José M. Cíes, Miguel López-Haro, Eloy del Río, José J. Calvino, and Prof. Serafín Bernal**
Departamento de Ciencia de los Materiales, Ingeniería Metalúrgica y Química Inorgánica, Facultad de Ciencias, Universidad de Cádiz, Campus Río San Pedro, E-11510 Puerto Real (Cádiz), Spain
E-mail: serafin.bernal@uca.es

♦ 2. Quantitative Estimate of Metal and Support Contributions to the CO Adsorbed on $Au/CeO_2–ZrO_2$ Catalysts

As revealed by the FTIR studies,[33] at 298 K under P(CO) ranging from 0 to 300 Torr, three major components contribute to the CO adsorption on Au/CZ catalysts. The first one due to CO adsorbed on Au(0) nanoparticles is characterized by a ν-CO stretching band typically occurring at about 2110 cm^{-1}.[18,20,30,32,34] The other two contributions are due to CO adsorbed on the support. They correspond to molecular forms weakly interacting with the CZ surface cations, whose characteristic ν-CO stretching bands are observed above 2143 cm^{-1},[52,53] and to carbonate-like species resulting from the strong interaction of CO with the surface anions of the support, respectively. The features characterizing the latter species appear at much lower wavenumbers, typically below 1700 cm^{-1}.[52,53] It is, therefore, critically important to develop an experimental approach allowing us to separate the three contributions above.

The key observation for developing such an approach came from FTIR studies of CO adsorption on a $Au/Ce_{0.62}Zr_{0.38}O_2$ catalyst prepared by deposition precipitation with urea and further activated at 523 K under flowing 5% O_2/He (Au/CZ).[33] Details of the preparation and activation routines are given in ref 33. The comparison of the spectra recorded at 298 K under P(CO) = 100 Torr and after 30 min evacuation at 298 K showed that the weak adsorbed forms, i.e., those corresponding to CO–Au and CO interacting with the surface Ce^{4+} and Zr^{4+} ions disappear, whereas bands assigned to the strongly adsorbed carbonate species remain practically unmodified.[33] If so, a volumetric adsorption routine consisting of two consecutive isotherms at 308 K separated by a 30 min evacuation at the same temperature would allow us to determine the specific contributions of the strong and weak adsorbed forms. Actually, the second isotherm would measure the joint contribution of the two weakly adsorbed forms, whereas the difference between the first and second isotherms would account for the strong, irreversible CO adsorption on the support.[41,42]

To separate the contributions of the weakly adsorbed forms due to the metal and support, the experimental routine applied to Au/CZ was also used in the investigation of the pure CZ sample.[41] By analogy with the interpretation proposed for the Au/CZ data, the second isotherm recorded for CZ would account for the CO weakly adsorbed on the support; therefore, the difference between the second isotherms for Au/CZ and CZ would measure the amount of CO specifically chemisorbed on the gold nanoparticles.[41]

Figure 1 summarizes an example of application to a Au/CZ powder catalyst of the routine discussed above.[42] In accordance with the difference isotherm (2–3) reported in part B of Figure 1, the experimental range of P(CO) at 308 K is wide enough as to reach the saturation coverage of gold. Similar results have also been reported for other samples of this family of powdered Au/CZ catalysts.[41]

Regarding the strong CO adsorption on the support, the difference isotherm (1–2) included in Figure 1, part B, suggests that an apparent saturation is also reached for P(CO) ≥ 50 Torr. Therefore, data reported in Table 1, all of them recorded at P(CO) = 100 Torr, may be considered to correspond to a saturated surface. In accordance with them, for this specific Au/CZ catalyst, CO strongly chemisorbed on the support is by far the largest contribution (78%), that due to the metal not exceeding the 17% of the total.

As will be discussed in the next sections, this approach provides a powerful tool for characterizing Au/CZ catalysts.

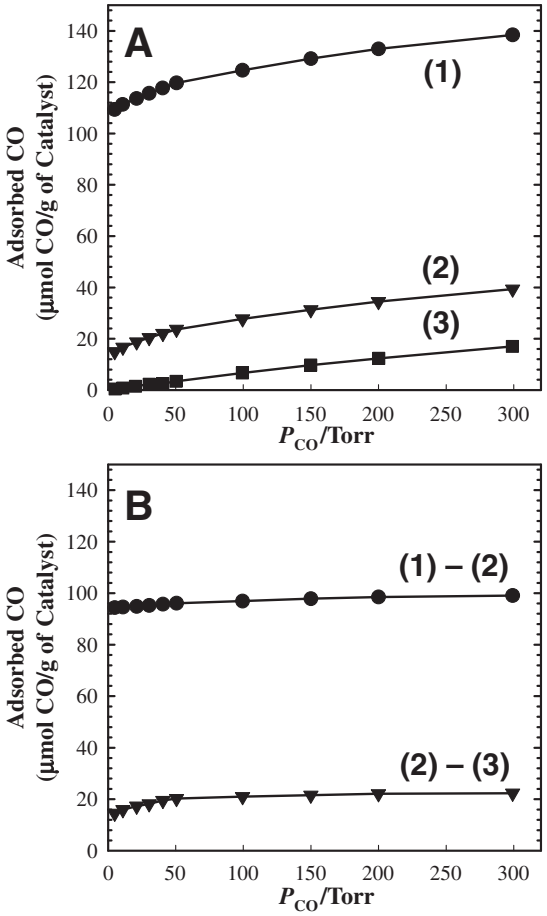

Figure 1. Application to a Au/CZ sample the approach for determining the metal and support contributions to the total amount of CO adsorbed on the catalyst. Part A) First (1) and second (2) isotherms for Au/CZ, and second isotherm for CZ (3). Part B) Difference isotherms resulting from the subtraction of those reported in Part A: (1) − (2), and (2) − (3). Isotherms recorded at 308 K. Some catalyst data: metal dispersion $D = Au_S/Au_T = 0.49$, and BET surface area: 63 $m^2 g^{-1}$. Reproduced with permission of Wiley-VCH from ref 42.

Table 1. Metal and support contributions to the CO adsorption on a Au/CZ catalyst as determined from the analysis of the volumetric data reported in Figure 1

	Separate contributions of Au and CZ (strong and weak forms)			
	CO–Au	CO–CZ (Strong)	CO–CZ (Weak)	Total
Adsorbed amount[a]	21	97	7	125

[a]Data (μmol CO $g^{-1}_{catalyst}$) at T = 308 K and P(CO) = 100 Torr.

From its application, rather detailed information about the relationship existing between chemical and nanostructural properties in this family of catalysts could be gained.

♦ 3. Nanostructural Analysis of the Au Sites for CO Adsorption

To have available quantitative data for CO specifically adsorbed on the metal in Au/CZ powder catalysts opens very interesting possibilities to the analysis of the nanostructural characteristics of the involved Au surface atoms. In fact, a procedure has recently been proposed for correlating CO adsorption data with the coordination number of the gold surface sites occurring in the investigated catalysts.[41] To do that, a model shape for the supported Au nanoparticles ought to be established.[41] On the basis of HRTEM studies,[41] a truncated cuboctahedron was proposed to be the most representative morphology among those experimentally observed in the investigated catalysts.[41] Computer simulation HRTEM imaging techniques gave further support to this proposal.[41] Though not based on HRTEM studies, a similar proposal has earlier been made for other supported gold catalysts.[40]

Figure 2 shows an example of model Au nanoparticle.[41] From its analysis, some typical parameters such as total number of atoms constituting the particle, Au_T, and the total number of surface atoms, Au_S, may easily be determined. Also very important, it is possible to evaluate the contribution to Au_S of atoms with the different coordination numbers (CN = j) occurring at the surface of the model particles, $Au_{S,j}$.

The approach developed in ref 41 implies four more steps, a) determination of the Au nanoparticle size distributions, as deduced from the analysis of experimental HRTEM and HAADF-STEM images recorded for the investigated catalysts; b) construction of a set of model nanoparticles covering the whole range of sizes observed in the experimental distributions; c) determination of the parameters, Au_T, Au_S, and $Au_{S,j}$, characterizing each of the members of the whole set of model nanoparticles; and d) development of a computer program allowing application to the experimental size distribution the nanostructural information previously generated for the surface atoms of the model nanoparticles. In this way, overall dispersion, $D = Au_S/Au_T$, data but also the contribution to D of surface atoms with a certain coordination number, CN = j, may be determined. This contribution will be hereafter referred to as $D_j = Au_{S,j}/Au_T$. The approach also allows us to determine the contribution to D of the Au atoms located at the perimeter of the metal/support interface, D_P. Likewise, the contribution of surface atoms with CN ranging from $j = m$ and $j = n$ may be easily determined as $D_{m-n} = \sum_{m-n} D_j$. Obviously, the extension of this equation to the whole range of observed CN values would measure the overall dispersion, D.

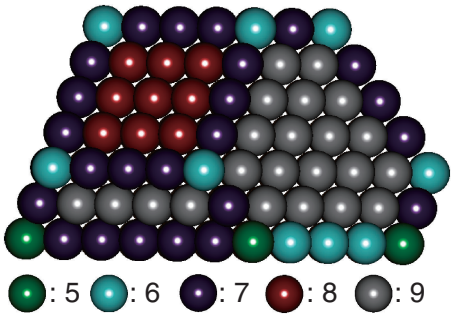

Figure 2. Example of Au model nanoparticle. Particle size: 2.9 nm. The color code accounts for the coordination number (CN) of its surface atoms.

This approach was first applied to two catalyst samples consisting of 2.5 wt % $Au/Ce_{0.62}Zr_{0.38}O_2$ (Au/CZ) and 1.5 wt % $Au/Ce_{0.50}Tb_{0.12}Zr_{0.38}O_2$ (Au/CTZ).[41] As deduced from Figure 3, these catalysts show different nanoparticle size distributions. Consistently with this, the sets of D_j, D_P, and D_{m-n} values determined for each of them, Table 2, are significantly different too.

If data reported in Table 2 are compared with the amounts of CO adsorbed on Au at saturation coverage, $P(CO) = 100$ Torr, as determined from the volumetric routine discussed above, $CO/Au_T = 0.49$ for Au/CZ and $CO/Au_T = 0.13$ for Au/CTZ, a number of interesting conclusions about the chemical properties of the supported gold phase could be drawn.[41]

First of all, $D = D_{4-9}$ values for Au/CZ, 0.69, and Au/CTZ, 0.29, are significantly larger than the corresponding CO/Au_T

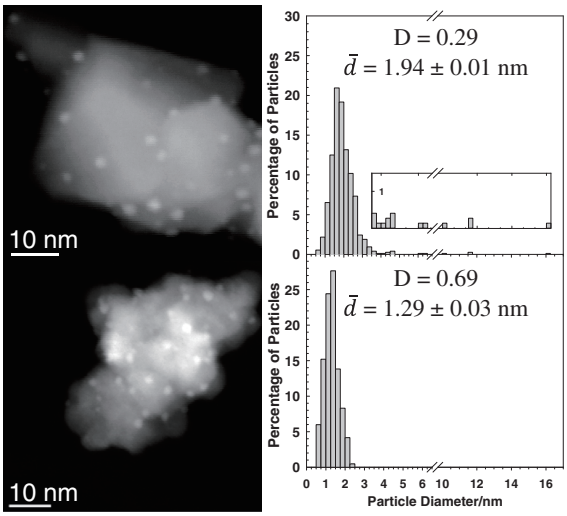

Figure 3. Representative HAADF-STEM images and Au nanoparticle size distributions for Au/CTZ (upper part) and Au/CZ (bottom part) catalysts.

Table 2. Contribution of Au surface atoms with CN = j to the metal dispersion in 2.5 wt % $Au/Ce_{0.62}Zr_{0.38}O_2$ (Au/CZ) and 1.5 wt % $Au/Ce_{0.50}Tb_{0.12}Zr_{0.38}O_2$ (Au/CTZ) catalysts as determined by application of the methodology developed in ref 41

Catalyst	D_4	D_5	D_6	D_7	D_8	D_9	D_P[a]
Au/CZ	0.02	0.07	0.17	0.22	0.01	0.20	0.17
Au/CTZ	0.00	0.02	0.05	0.07	0.02	0.13	0.06

Catalyst	D_{4-4}	D_{4-5}	D_{4-6}	D_{4-7}	D_{4-8}	D_{4-9}
Au/CZ	0.02	0.09	0.26	0.48	0.49	0.69
Au/CTZ	0.00	0.02	0.07	0.14	0.16	0.29

[a]Au atoms at the perimeter of metal/support interface showing a certain CN = j are included in the corresponding D_j values.

values. Therefore, in agreement with earlier studies on CO adsorption on gold[2,6,22,40] at saturation coverage, not all the surface atoms are active in the process. Moreover, the comparison of D_{4-j} values reported in Table 2 with the chemisorption data shows that the corresponding CO/Au_T and D_{4-7} data for both catalysts are in very good agreement. Therefore, under the applied experimental conditions, the surface saturation of gold particles is reached when sites with a well-defined nanostructure, i.e., those with $CN \leq 7$, are the only ones involved in the CO adsorption process.

By following a completely different approach, some quantitative studies of CO–Au adsorption in oxide-supported powder catalysts have earlier been reported.[31,54] However, a far less detailed description of the relationship existing between nanostructural properties of the Au surface atoms and their chemisorptive behavior could be deduced from them.

The interpretation suggested above is fully consistent with that proposed by Goodman et al.[9] for the same adsorption process on a Au(110) 1×2 reconstructed model surface at much lower temperature (100–250 K) and CO partial pressure (1×10^{-8}–1×10^{-4} Torr). As recently discussed,[41] this model surface actually consists of intersecting nanosized [111] planes in which sites with CN = 7 (25%), CN = 9 (50%), and CN = 11 (25%) coexist. Sites with CN = 7 would be responsible for the CO adsorption process. Accordingly, the chemical principles governing the CO–Au adsorption on both model single-crystal surfaces and conventional oxide-supported powder catalysts are essentially the same.[41] Obviously, some differences may be expected to exist between the model single-crystal and the nanoparticle gold surfaces. Thus, sites with $CN < 7$, not present in the model surface, may have a significant weight in the supported nanoparticles.[41] In effect, for Au/CTZ, sites with $CN \leq 6$ represent one fourth (24%) of the total surface atoms, this contribution becoming even larger, 38% in the case of Au/CZ, the catalyst showing the highest metal dispersion, Figure 3 and Table 2.[41] Likewise, the thermodynamics of the CO–Au adsorption and, therefore, the specific $P(CO)$-T relationship observed in a supported gold catalyst may depend on variables like the coordination number of the surface atoms,[6,9,13,55] the occurrence of some kind of metal/support interaction phenomenon,[14–16,23,43] and, though open to debate,[56] on quantum effects associated to the size of the metal nanoparticles.

♦ 4. Quantitative Study of CO Strongly Chemisorbed on the Support in Au/CZ Catalysts

The methodology discussed above has also been used for determining the amount of CO strongly chemisorbed on the support in two Au/CZ samples, hereafter referred to as Au/CZ-1 and Au/CZ-2. The metal loading (2.5 wt %), the CZ support, and the BET surface area ($63\ m^2\ g^{-1}$) were the same for both catalysts, the main difference between them being the Au nanoparticle size distributions, Figure 4.

As shown in part B of Figure 1, for a certain Au/CZ catalyst, the amount of CO strongly chemisorbed on the support is measured by the difference between the two consecutive isotherms recorded for it. Figure 5 summarizes the (1) − (2) difference isotherms for Au/CZ-1, Au/CZ-2, and the bare support (CZ), the latter being included for comparison.

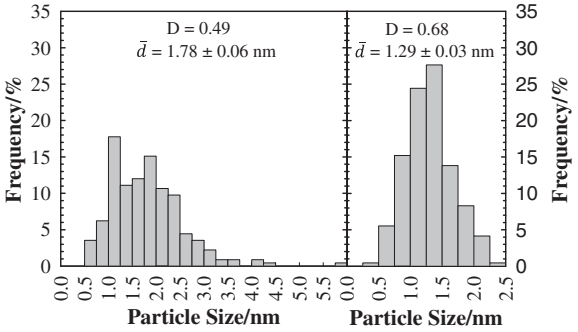

Figure 4. Au nanoparticle size distributions for Au/CZ-1 (left part) and Au/CZ-2 (right part) catalysts as determined from the analysis of HRTEM and HAADF-STEM images. Reproduced with permission of Wiley-VCH from ref 42.

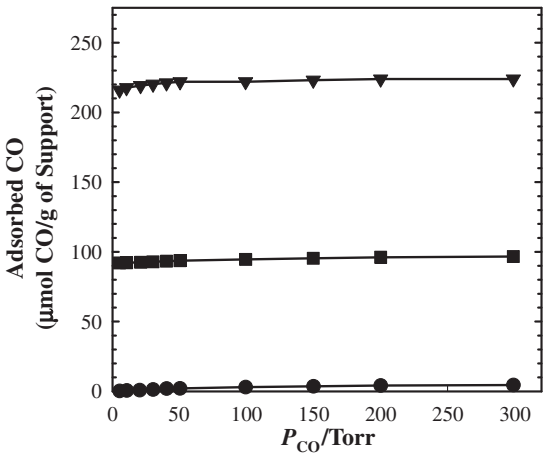

Figure 5. Volumetric study of the strong CO adsorption on CZ. Difference between the 1st and 2nd isotherms recorded at 308 K for the bare CZ support (●), Au/CZ-1 (■), and Au/CZ-2 (▼) samples. Reproduced with permission of Wiley-VCH from ref 42.

In accordance with Figure 5, at $P(CO) = 100$ Torr the amount of CO irreversibly chemisorbed on the support is found to be $6\ \mu mol\ g^{-1}_{sample}$ for the bare CZ oxide and much larger for the supported gold catalysts, $97\ \mu mol\ g^{-1}_{sample}$ for Au/CZ-1 and $220\ \mu mol\ g^{-1}_{sample}$ for Au/CZ-2. Also very remarkable is the difference observed between Au/CZ-1 and Au/CZ-2, particularly if it is recalled that the CZ support and the metal loading were the same for both catalysts.

A number of relevant conclusions could be drawn from this study.[42] a) The CO adsorption on the CZ support is kinetically controlled. b) The kinetics of the process is dramatically modified by the presence of gold, the Au nanoparticle size distribution shown by the catalysts playing also a very relevant role.[42] To our knowledge, no quantitative data evidencing such a strong influence of the metal phase on the chemical behavior of the oxide support had earlier been reported. Moreover, it is obvious from this study that the support contribution to the total amount of CO chemisorbed on Au/CZ catalysts cannot be determined from parallel adsorption studies carried out on the bare support.

The observations above clearly indicate that a mechanism implying the initial CO adsorption on the metal and its further transfer to the support (spillover) is much faster than the direct CO–CZ process.[42] Also interesting, the dependence of the CO adsorption on the Au nanoparticle size distribution suggests that the growth of the CO phase strongly chemisorbed on the support follows an annular model, the metal nanoparticles being located at the center of the annuli.[42] To confirm this proposal, the radius of these annuli (r_a) was estimated for Au/CZ-1 and Au/CZ-2 by application to the corresponding Au nanoparticle size distributions an adsorption model based on the following assumptions: a) r_a is constant and independent of the size of the Au nanoparticles; b) the surface of the support consists of [111] facets, the one showing the highest density of O^{2-} ions and thermodynamic stability;[57] and c) the adsorption process involves two surface O^{2-} sites per CO molecule.[42] The annulus radii thus determined for Au/CZ-1 and Au/CZ-2 were 1.9 and 1.7 nm, respectively.[42] Given the remarkable difference of Au nanoparticle size distribution shown by these two catalysts, the similarity of the annulus radius determined for them was considered to support the proposed model.[42]

♦ 5. Influence of the Redox State of the Support on the Chemical Properties of the Metal in Au/CZ Catalysts

The methodology developed in ref 41 could also be successfully applied to the quantification of the reversible metal deactivation effects occurred in a Au/CZ sample successively subjected to a series of treatments in which the support redox state was varied.[43] The starting point for this investigation consisted of a FTIR study of CO adsorbed on a single sample disk successively subjected to the following series of treatments: a) Heating in a flow of 5%O_2/He at 523 K (1 h), followed by 1 h evacuation at 523 K (Au/CZ-O523); b) After CO adsorption under P(CO) = 40 Torr at 298 K, the catalyst was evacuated at 298 K, subjected again to routine (a), then reduced in flow of 5%H_2/Ar at 473 K (1 h), and finally evacuated for 1 h at 473 K (Au/CZ-O523-R473); and c) Reoxidation by applying routine (a) to the catalyst resulting from the CO adsorption study on Au/CZ-O523-R473; this sample is referred to as Au/CZ-O523-R473-O523. Figure 6 summarizes the ν-CO spectra recorded for the three samples above.

As deduced from Figure 6, the spectrum for CO adsorbed on the supported Au nanoparticles is fully reversibly modified by the applied pretreatment and inherent to this by the support redox state.[43] Both the position, which is red-shifted from 2113 (spectra a and c) to 2101 cm^{-1} (spectrum b), and the integrated absorption (IA) of the band, which is approximately 15% lower for Au/CZ-O523-R473 (spectrum b) than for Au/CZ-O523 (spectrum a) and Au/CZ-O523-R473-O523 (spectrum c), are reversibly affected.

This experiment strongly suggests the likely occurrence of a strong metal/support interaction (SMSI) effect, as originally defined by Tauster et al.,[58] i.e., the CO adsorption capability of the gold nanoparticles may be reversibly modified as a function of the redox state of the support.

To confirm the proposal above, a number of additional studies were performed.[43] The metal nanoparticle size distributions for the three catalysts above were determined by HRTEM and HAADF-STEM techniques. It was found that, within the experimental error,[41] neither D (=D_{4-9}) nor D_{4-7} parameters as earlier defined[41] (see also Section **3** of this work) were modified throughout the whole series of applied pretreatments. This allowed the authors to exclude eventual metal sintering and redispersion effects as the likely origin of the changes observed in the FTIR spectra.

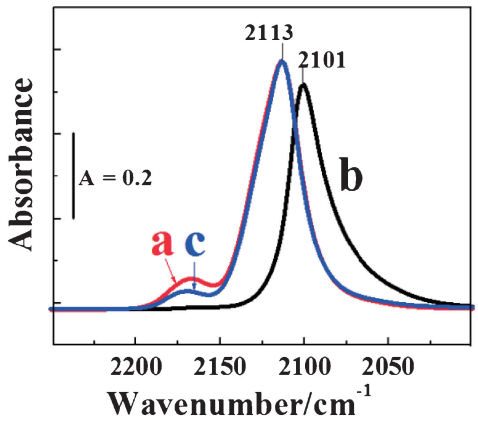

Figure 6. FTIR study of CO adsorbed on a Au/CZ catalyst successively subjected to the following pretreatment routines: a) O523; b) O523-R473); and c) O523-R473-O523. Spectra recorded at 298 K, under P(CO) = 40 Torr. Reproduced with permission of Wiley-VCH from ref 43.

Likewise, by applying the methodology developed in ref 41, the amount of CO specifically chemisorbed on the metal nanoparticles could be determined for the three catalysts. The volumetric study was performed on the same sample successively subjected to the series of pretreatments described above. The corresponding data at P(CO) = 40 Torr, the partial pressure used in the FTIR study reported in Figure 6, were found to be 19.4, 10.9, and 19.3 $\mu mol\ g^{-1}_{catalyst}$, for Au/CZ-O523, Au/CZ-O523-R473, and Au/CZ-O523-R473-O523, respectively. These results fully confirm the occurrence of reversible changes in the CO adsorption capability of the supported gold phase. These changes were interpreted as due to parallel modifications in the electronic structure of the metal nanoparticles.[43] In particular, the deactivation effect observed in the Au/CZ-O523-R473 sample was proposed to be caused by electron-transfer phenomena occurring from the reduced support to the Au nanoparticles.[43] This proposal is consistent with the reversible changes that occur in the Au 4f XP spectrum upon applying the successive series of pretreatments to the Au/CZ catalyst.[43]

The comparison of the changes induced by the O523-R473 pretreatment on the IA of the ν-CO–Au band and the amount of CO adsorbed on Au, as determined from the volumetric studies, is also interesting. As already mentioned, the IA value for the reduced catalyst (Au/CZ-O523-R473) is a 15% lower than those determined for Au/CZ-O523 and Au/CZ-O523-R473-O523, the samples presenting a fully oxidized support. In the case of the volumetric study, the relative effect is much stronger, a decrease of 44% of the CO adsorption capability being observed. This allowed the authors to conclude that the absorption coefficient for the ν-CO–Au band is sensitive to the redox state of the support, it being larger for the metal under the

SMSI state. This in turns means that FTIR spectroscopy should be carefully used in quantitative analysis of the strong metal/support interaction effects eventually occurring in Au/CZ catalysts.

♦ 6. Conclusion

A methodology recently developed for characterizing the chemical properties of Au/CZ and closely related catalysts is briefly reviewed. The approach combines conventional FTIR and volumetric studies of CO adsorption with experimental HRTEM and HAADF-STEM studies, HRTEM image simulation, and computer modeling nanostructural techniques. Despite the difficulties for using CO adsorption as a tool for characterizing Au/CZ catalysts, this approach is shown to provide very fine details about the chemical behavior of this family of catalysts.

In addition to briefly analyzing the chemical principles governing the approach, three major aspects of the CO–(Au/CZ) interaction could be discussed on a quantitative basis.

Regarding the CO adsorption on Au, a correlation could be established between the adsorbed amount and the nanostructural properties of the surface metal atoms.[41] At saturation coverage, CO adsorption occurs on sites with CN ≤ 7. This observation actually bridges the T and P(CO) gap existing between the adsorption studies carried out on Au single-crystal surfaces and supported nanoparticles. Provided that nanoparticle size distributions are known, this methodology not only allows us to interpret CO adsorption data, but also very promising, it opens a way to make predictions about the chemisorptive behavior of supported gold phases and even to analyze on a finer nanostructural basis CO oxidation data like those recently discussed in ref 59.

It has also been shown that the supported gold phase strongly modifies the irreversible adsorption of CO on CZ supports.[42] Moreover, a model correlating the amount of this adsorbed form and the Au nanoparticle size distribution could be proposed.[43] This model suggests an annular growth of the adsorbed phase around the Au nanoparticles, the radius of the resulting annuli being 2 nm approximately.[42] This is relevant information in analysis of activity data and catalyst deactivation effects.

Finally, the developed methodology has been used to show the occurrence of a SMSI-like effect in Au/CZ catalysts: a conclusion with obvious and very relevant implications in the analysis of activity data for reactions occurring under net reducing conditions.[43]

This work has been supported by MICIIN-Spain/FEDER-EU (MAT2008-00889-NAN) and the *Junta de Andalucía* (FQM-110 and FQM-334).

References

1 M. Haruta, T. Kobayashi, H. Sano, N. Yamada, *Chem. Lett.* **1987**, 405.
2 G. C. Bond, C. Louis, D. T. Thompson, *Catalysis by Gold*, Imperial College Press, London, **2006**, p. 161.
3 G. C. Bond, D. T. Thompson, *Catal. Rev.–Sci. Eng.* **1999**, *41*, 319.
4 G. J. Hutchings, *Dalton Trans.* **2008**, 5523.
5 L. C. Wang, H. J. Jin, D. Widmann, J. Weissmüller, R. J. Behm, *J. Catal.* **2011**, *278*, 219.
6 R. Meyer, C. Lemire, Sh. K. Shaikhutdinov, H.-J. Freund, *Gold Bull.* **2004**, *37*, 72.
7 S. A. C. Carabineiro, B. E. Nieuwenhuys, *Gold Bull.* **2009**, *42*, 288.
8 J. M. Gottfried, K. J. Schmidt, S. L. M. Schroeder, K. Christmann, *Surf. Sci.* **2003**, *536*, 206.
9 D. C. Meier, V. Bukhtiyarov, D. W. Goodman, *J. Phys. Chem. B* **2003**, *107*, 12668.
10 L. Piccolo, D. Loffreda, F. J. C. S. Aires, C. Deranlot, Y. Jugnet, P. Sautet, J. C. Bertolini, *Surf. Sci.* **2004**, *566–568*, 995.
11 J. Kim, E. Samano, B. E. Koel, *J. Phys. Chem. B* **2006**, *110*, 17512.
12 C. J. Weststrate, E. Lundgren, J. N. Andersen, E. D. L. Rienks, A. C. Gluhoi, J. W. Bakker, I. M. N. Groot, B. E. Nieuwenhuys, *Surf. Sci.* **2009**, *603*, 2152.
13 D. C. Meier, D. W. Goodman, *J. Am. Chem. Soc.* **2004**, *126*, 1892.
14 B. Yoon, H. Häkkinen, U. Landman, A. S. Wörz, J.-M. Antonietti, S. Abbet, K. Judai, U. Heiz, *Science* **2005**, *307*, 403.
15 A. S. Wörz, U. Heiz, F. Cinquini, G. Pacchioni, *J. Phys. Chem. B* **2005**, *109*, 18418.
16 M. Sterrer, M. Yulikov, T. Risse, H.-J. Freund, J. Carrasco, F. Illas, C. Di Valentin, L. Giordano, G. Pacchioni, *Angew. Chem., Int. Ed.* **2006**, *45*, 2633.
17 M. Sterrer, M. Yulikov, E. Fischbach, M. Heyde, H.-P. Rust, G. Pacchioni, T. Risse, H.-J. Freund, *Angew. Chem., Int. Ed.* **2006**, *45*, 2630.
18 M. Chen, D. W. Goodman, *Acc. Chem. Res.* **2006**, *39*, 739.
19 T. Diemant, H. Hartmann, J. Bansmann, R. J. Behm, *J. Catal.* **2007**, *252*, 171.
20 T. Risse, S. Shaikhutdinov, N. Nilius, M. Sterrer, H.-J. Freund, *Acc. Chem. Res.* **2008**, *41*, 949.
21 M. Baron, O. Bondarchuk, D. Stacchiola, S. Shaikhutdinov, H.-J. Freund, *J. Phys. Chem. C* **2009**, *113*, 6042.
22 C. J. Weststrate, A. Resta, R. Westerström, E. Lundgren, A. Mikkelsen, J. N. Andersen, *J. Phys. Chem. C* **2008**, *112*, 6900.
23 C. J. Weststrate, R. Westerström, E. Lundgren, A. Mikkelsen, J. N. Andersen, A. Resta, *J. Phys. Chem. C* **2009**, *113*, 724.
24 K. T. Rim, D. Eom, L. Liu, E. Stolyarova, J. M. Raitano, S.-W. Chan, M. Flytzani-Stephanopoulos, G. W. Flynn, *J. Phys. Chem. C* **2009**, *113*, 10198.
25 Y. Iizuka, H. Fujiki, N. Yamauchi, T. Chijiiwa, S. Arai, S. Tsubota, M. Haruta, *Catal. Today* **1997**, *36*, 115.
26 F. Boccuzzi, A. Chiorino, M. Manzoli, D. Andreeva, T. Tabakova, *J. Catal.* **1999**, *188*, 176.
27 F. Boccuzzi, A. Chiorino, M. Manzoli, P. Lu, T. Akita, S. Ichikawa, M. Haruta, *J. Catal.* **2001**, *202*, 256.
28 M. Manzoli, A. Chiorino, F. Boccuzzi, *Surf. Sci.* **2003**, *532–535*, 377.
29 S. Derrouiche, P. Gravejat, D. Bianchi, *J. Am. Chem. Soc.* **2004**, *126*, 13010.
30 P. Concepción, S. Carrettin, A. Corma, *Appl. Catal., A* **2006**, *307*, 42.
31 F. Menegazzo, M. Manzoli, A. Chiorino, F. Boccuzzi, T.

Tabakova, M. Signoretto, F. Pinna, N. Pernicone, *J. Catal.* **2006**, *237*, 431.
32 M. Manzoli, F. Boccuzzi, A. Chiorino, F. Vindigni, W. Deng, M. Flytzani-Stephanopoulos, *J. Catal.* **2007**, *245*, 308.
33 S. E. Collins, J. M. Cíes, E. del Río, M. López-Haro, S. Trasobares, J. J. Calvino, J. M. Pintado, S. Bernal, *J. Phys. Chem. C* **2007**, *111*, 14371.
34 F. Vindigni, M. Manzoli, A. Chiorino, F. Boccuzzi, *Gold Bull.* **2009**, *42*, 106.
35 W. T. Wallace, R. L. Whetten, *J. Phys. Chem. B* **2000**, *104*, 10964.
36 A. Fielicke, G. von Helden, G. Meijer, B. Simard, D. M. Rayner, *J. Phys. Chem. B* **2005**, *109*, 23935.
37 A. Fielicke, G. von Helden, G. Meijer, D. B. Pedersen, B. Simard, D. M. Rayner, *J. Am. Chem. Soc.* **2005**, *127*, 8416.
38 M. Okumura, Y. Kitagawa, M. Haruta, K. Yamaguchi, *Appl. Catal., A* **2005**, *291*, 37.
39 C. Zhang, A. Michaelides, S. J. Jenkins, *Phys. Chem. Chem. Phys.* **2011**, *13*, 22.
40 T. V. W. Janssens, B. S. Clausen, B. Hvolbæk, H. Falsig, C. H. Christensen, T. Bligaard, J. K. Nørskov, *Top. Catal.* **2007**, *44*, 15.
41 M. López-Haro, J. J. Delgado, J. M. Cies, E. del Rio, S. Bernal, R. Burch, M. A. Cauqui, S. Trasobares, J. A. Pérez-Omil, P. Bayle-Guillemaud, J. J. Calvino, *Angew. Chem., Int. Ed.* **2010**, *49*, 1981.
42 J. M. Cíes, J. J. Delgado, M. López-Haro, R. Pilasombat, J. A. Pérez-Omil, S. Trasobares, S. Bernal, J. J. Calvino, *Chem.—Eur. J.* **2010**, *16*, 9536.
43 J. M. Cíes, E. del Río, M. López-Haro, J. J. Delgado, G. Blanco, S. Collins, J. J. Calvino, S. Bernal, *Angew. Chem., Int. Ed.* **2010**, *49*, 9744.
44 D. Tibiletti, A. Amieiro-Fonseca, R. Burch, Y. Chen, J. M. Fisher, A. Goguet, C. Hardacre, P. Hu, D. Thompsett, *J. Phys. Chem. B* **2005**, *109*, 22553.
45 A. A. Fonseca, J. M. Fisher, D. Ozkaya, M. D. Shannon, D. Thompsett, *Top. Catal.* **2007**, *44*, 223.
46 S.-P. Wang, T.-Y. Zhang, X.-Y. Wang, S.-M. Zhang, S.-R. Wang, W.-P. Huang, S.-H. Wu, *J. Mol. Catal. A: Chem.* **2007**, *272*, 45.
47 F. C. Meunier, A. Goguet, C. Hardacre, R. Burch, D. Thompsett, *J. Catal.* **2007**, *252*, 18.
48 A. Goguet, R. Burch, Y. Chen, C. Hardacre, P. Hu, R. W. Joyner, F. C. Meunier, B. S. Mun, D. Thompsett, D. Tibiletti, *J. Phys. Chem. C* **2007**, *111*, 16927.
49 I. Dobrosz-Gómez, I. Kocemba, J. M. Rynkowski, *Appl. Catal., B* **2008**, *83*, 240.
50 I. Dobrosz-Gómez, I. Kocemba, J. M. Rynkowski, *Catal. Lett.* **2009**, *128*, 297.
51 H. Daly, A. Goguet, C. Hardacre, F. C. Meunier, R. Pilasombat, D. Thompsett, *J. Catal.* **2010**, *273*, 257.
52 M. Daturi, C. Binet, J.-C. Lavalley, A. Galtayries, R. Sporken, *Phys. Chem. Chem. Phys.* **1999**, *1*, 5717.
53 M. Daturi, C. Binet, J. C. Lavalley, G. Blanchard, *Surf. Interface Anal.* **2000**, *30*, 273.
54 A. Chiorino, M. Manzoli, F. Menegazzo, M. Signoretto, F. Vindigni, F. Pinna, F. Boccuzzi, *J. Catal.* **2009**, *262*, 169.
55 C. Lemire, R. Meyer, Sh. K. Shaikhutdinov, H.-J. Freund, *Surf. Sci.* **2004**, *552*, 27.
56 C. Lemire, R. Meyer, Sh. Shaikhutdinov, H.-J. Freund, *Angew. Chem., Int. Ed.* **2004**, *43*, 118.
57 M. Nolan, S. Grigoleit, D. C. Sayle, S. C. Parker, G. W. Watson, *Surf. Sci.* **2005**, *576*, 217.
58 S. J. Tauster, S. C. Fung, R. L. Garten, *J. Am. Chem. Soc.* **1978**, *100*, 170.
59 I. X. Green, W. Tang, M. Neurock, J. T. Yates, Jr., *Science* **2011**, *333*, 736.

